



King's Research Portal

DOI:

[10.1111/ajt.13617](https://doi.org/10.1111/ajt.13617)

Document Version

Peer reviewed version

[Link to publication record in King's Research Portal](#)

Citation for published version (APA):

Taubert, R., Danger, R. A. E. D., Londono, M-C., Christakoudi, S., Martinez-Picola, M., Rimola, A., Manns, M., Sanchez Fueyo, A., & Jaeckel, E. (2016). Hepatic Infiltrates in Operational Tolerant Patients After Liver Transplantation Show Enrichment of Regulatory T Cells Before Proinflammatory Genes Are Downregulated. *American Journal of Transplantation*. <https://doi.org/10.1111/ajt.13617>

Citing this paper

Please note that where the full-text provided on King's Research Portal is the Author Accepted Manuscript or Post-Print version this may differ from the final Published version. If citing, it is advised that you check and use the publisher's definitive version for pagination, volume/issue, and date of publication details. And where the final published version is provided on the Research Portal, if citing you are again advised to check the publisher's website for any subsequent corrections.

General rights

Copyright and moral rights for the publications made accessible in the Research Portal are retained by the authors and/or other copyright owners and it is a condition of accessing publications that users recognize and abide by the legal requirements associated with these rights.

- Users may download and print one copy of any publication from the Research Portal for the purpose of private study or research.
- You may not further distribute the material or use it for any profit-making activity or commercial gain
- You may freely distribute the URL identifying the publication in the Research Portal

Take down policy

If you believe that this document breaches copyright please contact librarypure@kcl.ac.uk providing details, and we will remove access to the work immediately and investigate your claim.

This is the peer reviewed version of the following article:

Hepatic infiltrates in operational tolerant patients after liver transplantation show enrichment of regulatory T cells before proinflammatory genes are down-regulated,

which has been published in final form at

<http://onlinelibrary.wiley.com/doi/10.1111/ajt.13617/abstract>

This article may be used for non-commercial purposes in accordance with
[Wiley Terms and Conditions for Self-Archiving](#)

<http://olabout.wiley.com/WileyCDA/Section/id-820227.html#terms>

Hepatic infiltrates in operational tolerant patients after liver transplantation show enrichment of regulatory T cells before proinflammatory genes are down-regulated

#Richard Taubert^{1, 2}, #Richard Danger³, María-Carlota Londoño⁴, Sofia Christakoudi^{5, 6}, Marta Martinez⁴, Antoni Rimola³, Michael P. Manns¹, *Alberto Sánchez-Fueyo^{3, 4}, *Elmar Jaeckel^{1, 2}

¹ Department of Gastroenterology, Hepatology and Endocrinology, Hannover Medical School, Hannover, Germany

² Integrated Research and Treatment Center Transplantation (IFB-Tx), Hannover Medical School, Hannover, Germany

³ Institute of Liver Studies, Liver Sciences Department, MRC Centre for Transplantation, School of Life Sciences & Medicine, King's College London University, King's College Hospital, Denmark Hill, London, SE5 9RS, UK.

⁴ Liver Unit, Hospital Clinic Barcelona, IDIBAPS, CIBEREHD, University of Barcelona, Barcelona, Spain

⁵ Department of Biostatistics, IoPPN King's College London, London, United Kingdom

⁶ Department of Experimental Immunobiology, MRC Centre for Transplantation, King's College London, London, United Kingdom

equal first authors; * equal senior authors

Running title: Immune regulation in tolerant liver grafts

Keywords: spontaneous operational tolerance, regulatory T cell, FOXP3, human, rejection, liver transplantation.

Correspondence should be addressed to:

Elmar Jaeckel, MD

Dept. of Gastroenterology, Hepatology & Endocrinology

Hannover Medical School

Carl-Neuberg-Str. 1

30625 Hannover

Germany

Phone +49-511-532 9513

Fax +49-511-532 6998

E-mail: Jaeckel.elmar@mh-hannover.de

Alberto Sanchez-Fueyo

Institute of Liver Studies

King's College Hospital

MRC Transplant Centre

Faculty of Life Sciences and Medicine

King's College London

Denmark Hill

London SE59RS

United Kingdom

Phone +44-2032993305

Fax +44-2032993760

E-mail: sanchez_fueyo@kcl.ac.uk

Abbreviations:

ACR: acute cellular rejection; FFPE: formalin fixed paraffin embedded; HCV: Hepatitis C virus; IS: immunosuppression; SOT: spontaneous operational tolerance; Teff: effector T cells; Tregs: regulatory T cells; TSDR: Treg-specific demethylated region

Abstract

Immunosuppression can be discontinued from selected and stable patients after liver transplantation resulting in spontaneous operational tolerance (SOT), although the underlying mechanisms remain elusive. Thus we analyzed serial liver biopsies from adult liver recipients enrolled in a prospective multi-center immunosuppression withdrawal trial employing immunophenotyping and transcriptional profiling. Liver samples were collected before the initiation of weaning, at time of rejection, or 1 and 3 years after complete drug discontinuation. Unexpectedly the tolerated grafts developed portal tract expansion with increased T cell infiltration after immunosuppression withdrawal. This was associated with transient and preferential accumulation of CD4⁺FOXP3⁺ cells and a trend towards up-regulation of immune activation and regulatory genes, without signs of rejection. At the same time no markers of endothelial damage or activation were noted. Portal infiltrates persisted at 3 year, but were characterized by decreased expression of genes associated with chronic immunological damage. Furthermore SOT was not associated with a progressive liver fibrosis up to five years. These data suggest that SOT involves several mechanisms: a long-lasting local immune cell persistence with a transient regulatory T cells accumulation followed by a down-regulation of immune activated genes over years. These results have important implications for designs and follow-up of weaning trials.

Introduction

Most human liver transplant recipients require lifelong immunosuppression (IS) to prevent immune-mediated graft damage, which is associated with relevant clinical complications like infection, malignancies, renal dysfunction and metabolic disturbances, that contribute to the stagnation of long term survival outcomes (1). Years after transplantation, however, selected liver recipients can discontinue IS and maintain normal graft function, a phenomenon known as spontaneous operational tolerance (SOT)(2). Liver transplantation exhibits lower graft loss from rejection episodes and by far the highest rates of SOT as compared with other solid organ transplantation settings (2-4). The immune privileged status of liver allografts is even more clearly displayed in animal models (*e.g.* mice, rats, dogs and pigs), in which the default outcome of allogeneic liver transplantation in the absence of IS tends to be spontaneous acceptance rather than rejection (5-7). The mechanisms responsible for allograft tolerance in these models are not completely understood, but lack of immune response against the liver is clearly not the cause. Instead, the allogeneic liver rapidly activates alloreactive T cells, which then infiltrate the graft and induce pathologic changes resembling mild rejection. This is followed by deletion of the activated alloreactive T cells via apoptosis or emperipolesis, and generation of regulatory T cells (Tregs), which restore homeostasis and establish donor-specific tolerance (8). Whether similar mechanisms are responsible for the development of SOT in human transplantation is unknown.

Studies focused on the characterization of SOT patients identified changes in both peripheral blood and liver tissue. Thus, as compared with patients under maintenance IS, SOT patients displayed increased numbers of circulating CD4⁺CD25⁺ Tregs, $\gamma\delta$ T cells, and a higher ratio of V δ 1/V δ 2 or pDC2/pDC1 cells

(9-14). Likewise some studies reported that liver biopsies of SOT patients contained more FOXP3⁺ cells than patients under IS (15, 16).

Two recent prospective IS withdrawal trials in selected adult and pediatric patients, respectively, have been particularly informative, demonstrating that SOT is more prevalent than previously estimated (40 to 60% of enrolled patients)(17-19), but only in patients in whom IS withdrawal is attempted late after transplantation. Furthermore, at least in adults, successful IS withdrawal is also independently associated with recipient age. These data suggest that gradual attrition of the alloreactive T cell pool over several years through exhaustion/senescence may be required to achieve SOT. The adult study also revealed that the use of intrahepatic transcriptional biomarkers predicted the outcome of IS withdrawal (17) much more accurately than any combination of peripheral blood biomarkers. The need to study the graft as opposed to blood is further emphasized by the observation that during acute cellular rejection (ACR) Treg frequencies are differentially regulated between blood (reduced/normal) and liver allografts (increased) (20, 21), and that in a humanized mouse model the ability of Tregs to home into the allograft is indispensable to induced tolerance (22).

To investigate the immune regulatory mechanisms elicited by IS withdrawal, in the current study we longitudinally analyzed the distribution of intrahepatic T cell subsets and gene expression patterns in protocol liver biopsies obtained from operationally tolerant liver recipients before, 1 and 3 years after successful IS withdrawal.

Materials and Methods

Subjects

Biological samples were obtained from liver recipients enrolled in a previously reported prospective multicenter trial of IS withdrawal (clinicaltrials.gov identification NCT00647283) (17, 18). Briefly, IS doses were gradually decreased until complete discontinuation over 6-9 months. Patients were then followed-up for 60 additional months. Protocol liver biopsies were obtained in all patients at baseline (before IS withdrawal), 1 and 3 years and in a subgroup at 5 years after successful drug withdrawal (in SOT recipients), and at the time of rejection (in non-tolerant recipients). Patients who did not develop rejection were classified as SOT as long as IS cessation was maintained for at least 12 months with stable liver function and no histopathologic evidences of acute and/or chronic rejection. Out of the 102 recipients participating in the trial, IS withdrawal was successful in 41 recipients. For the current study, we selected a subgroup of 24 SOT recipients from whom sequential liver biopsies and blood samples were available for immune phenotype (n=18 for immunohistology and 12/18 for additional flow cytometry) and/or transcriptional (n=17) analyses (Suppl. Tab. 1). Gene expression analyses, were also performed in a group of 14 non-tolerant recipients before IS withdrawal and while undergoing rejection. Only hepatitis C virus (HCV) negative patients enrolled at Hospital Clinic Barcelona were employed for these analyses. Characteristics and clinical data of patients whose samples were employed are summarized in Table 1. This study was approved by the local research Ethics Committee of all participating institutions and written informed consent was obtained from each patient.

Liver biopsy specimens

Liver biopsies were performed percutaneously under local anesthesia. A 2- to 3-mm portion of the needle biopsy was immediately preserved in RNAlater reagent (Ambion), kept at 4°C for 24 hours, and then at -80°C after removal of the RNAlater. The remaining cylinder was formalin fixed and paraffin embedded (FFPE).

Histological assessment of liver biopsies

For histological assessment, 3- μ m thick slides were stained using hematoxylin and eosin, Masson's trichrome for connective tissue analysis. All histo-pathological examinations were performed by the same pathologist, who was blinded to all clinical and biological data.

Immunohistological methods

Intrahepatic immunophenotyping was performed as previously published (17, 20, 23). We determined the portal infiltrate size by encircling portal infiltrates along the limiting plate and excluded the lumen of veins, arteries and bile ducts (Fig. 1A).

We histologically analyzed the intrahepatic infiltration of CD4⁺CD8⁻FOXP3⁻ (CD4⁺), CD8⁺CD4⁻FOXP3⁻ (CD8⁺), CD4⁺CD8⁻FOXP3⁺ (CD4⁺FOXP3⁺ Tregs) and CD8⁺CD4⁻FOXP3⁺ (CD8⁺FOXP3⁺) cells (Fig. 1). In the current study 96.1% of portal FOXP3⁺ cells were CD4⁺, and only 3.9% were potentially activated CD8⁺FOXP3⁺ Teff, excluding a significant contamination of activated Teff in the pool of CD4⁺FOXP3⁺ Tregs. The Treg detection via immunofluorescence of human FFPE tissue was recently validated by employing flow cytometry and epigenetic analysis(20, 23).

Flow cytometry

Flow cytometry immunophenotyping of whole blood samples was performed in a subset of 12 recipients from whom sequentially collected specimens were available (17). Titrated amounts of fluorochrome-conjugated monoclonal antibodies were employed to identify CD4⁺ and CD8⁺ T cells and Tregs (Suppl. Fig 1, Tab. 3). Cells were fixed in 1% paraformaldehyde/PBS, and data were acquired on a BD FACSCanto (BD) and analyzed employing FlowJo software (Tree Star).

Liver tissue RNA extraction and processing

Total RNA were extracted according to the TRIzol manufacturer's protocol (Invitrogen). Quality and quantity were assessed with the Agilent 2100 Bioanalyzer (Agilent Technologies) and Nanodrop ND-1000, respectively. DNA was removed from total RNA preparations using Turbo DNA-free DNase treatment (Ambion) and RNA was then reverse transcribed into cDNA using the High-Capacity cDNA Reverse Transcription Kit (Applied Biosystems). Gene lists were taken from our previous publication and the published results of the "Molecular Microscope System" from the "Alberta Transplant Applied Genomic Centre" (<http://atagc.med.ualberta.ca/Research/GeneLists/Pages/default.aspx>) (17, 24). A pre-amplification of cDNA over 10 cycles was performed using pooled TaqMan Assays and the TaqMan PreAmp Master Mix following manufacturer's protocol. qPCR was performed using the 48.48 Dynamic Array following manufacturer's protocol using a BioMark (both Fluidigm Corporation, CA, USA). To quantify transcript levels, target gene Ct values were normalized using Ct values of HPRT1 as a reference gene to generate $-\Delta\text{Ct}$ values.

Statistical analysis

Statistical analysis was performed in R (<http://www.R-project.org>). Sequential samples from SOT patients were compared using linear mixed-effects models (*nlme* package) with a random effect for intercept. This approach accounted for repeated measurements and for missing data. The study design was balanced with data collected at similar time-points but complete datasets for all time-points were not available in all patients (Suppl. Tab. 1). A global p-value derived from likelihood ratio test was used to evaluate the total effect of time for each model. Extreme outliers were detected using Bonferroni outlier test (*car* package) and were re-coded to the next highest or next lowest value in the corresponding time-point group depending on the direction of the extreme value. For the analysis of *Infiltrate Size* data were log transformed (ln) to account for a skewed distribution at 3 years SOT. Bonferroni correction was used to adjust p-values derived from multiple comparisons.

Comparison between paired pre-weaning and rejector samples was performed with paired t-tests using GraphPad Prism 6 software. Fold-differences for gene expression data were calculated according to the comparative C_T method ($2^{-\Delta\Delta C_T}$ method). P-values <0.05 (two-tailed) were considered statistically significant in all analyses.

Results

The development of operational tolerance is currently being tested in several clinical trials. In order to gain a better understanding of the mechanisms of operational tolerance, we evaluated serial liver biopsies of tolerant patients for composition of the immune infiltrates (Fig. 1). Furthermore, to elucidate the functional aspects of intrahepatic immune responses the quantitative immunophenotypic analysis was paralleled by intrahepatic gene expression analysis.

To our surprise we detected increased portal infiltrates one and three years after complete IS withdrawal in patients with normal transaminases (Fig. 2A). We already reported on mild portal inflammation and lymphocytic cholangitis at one year in our previous analysis (18). However, the current quantitative analysis revealed significant changes one and three years of SOT (Fig. 1A, Fig. 2A, Table. 2). These changes were significantly milder than those observed in non-tolerant recipients at the time of rejection and did not fulfill Banff criteria for rejection. Furthermore, portal infiltrate size was associated with the elapsed time post-withdrawal ($p=0.002$) (Tab. 2, Fig. 2A). The assessment of portal tract expansion by conventional semi-quantitative histological scores was too insensitive to detect these longitudinal differences (Suppl. Tab. 2).

Longer follow-up liver biopsies at 5 years SOT were only available in a subgroup of 5 patients (Suppl. Tab. 1). The progression of the fibrosis score (F1 to F2) from 3 to 5 years post withdrawal was noted in 1 patient, although this was not associated with increased portal or lobular inflammatory infiltrates. No changes in fibrosis were noted in the remaining 4 patients in this time interval. Furthermore anti-donor HLA antibodies, that were assessed in about 80% of the patients in the initial study (18), were only detectable in 3 tolerant patients with sequential liver

biopsies.

T cells accumulated in the portal tracts and were almost absent in the liver lobules. Longitudinal analyses of the portal T cell infiltration showed a significant accumulation of CD4⁺FOXP3⁺ Tregs expressed as the portal Treg density at 1 year SOT (Fig. 2B) with a significant reduction of the portal Treg/CD4⁺ and Treg/CD4⁺+CD8⁺ ratios from 1 year to 3 years SOT (Fig. 2C, Tab. 2). The CD4⁺ and CD8⁺ effector T cell densities varied insignificantly (Fig. 2D). However, we noticed a trend to an increased CD4⁺/CD8⁺ ratio at 3 years SOT, which is a marked contrast to the decreased CD4⁺/CD8⁺ ratio observed during ACR (20). The longitudinal changes of portal T cell infiltration pattern were not reflected by the longitudinal changes in all available blood samples underlining the importance to study cellular and molecular changes directly in the graft (Tab. 3, Suppl. Fig. 1, Fig. 2E).

As liver cell immunohenotyping does not allow us to draw functional conclusions, we complemented the data with transcript levels of a set of 48 genes known to be involved in allograft rejection, immune regulation, and graft endothelium activation/damage (24) (Table 4). Analysis of liver samples obtained from tolerant recipients before and after successful IS-withdrawal revealed significant changes in pro-inflammatory, immune regulatory and endothelial-related genes (Table 4, Fig 3, Suppl. Tab. 3).

The expression of *FOXP3* followed the same pattern as the portal CD4⁺FOXP3⁺ Tregs in the immunohistology analyses, with a significant transient increase at 1 year post-drug withdrawal, and a subsequent return to the pre-weaning levels at 3 years post-withdrawal ($p=0.013$ and 0.003 , respectively) (Fig. 3A). Two other immune regulatory genes, *PD1* and *BATF*, showed a non-significant increase in

expression at 1 year post-withdrawal followed by a significantly decreased expression at 3 years SOT (Table 4, Suppl. Tab. 3).

From 20 rejection-associated genes analyzed, only *IL32* transcript levels significantly increased 1-year post-withdrawal as compared with baseline (Fig. 3B). In contrast, all other genes known to be associated with rejection were not significantly increased or their expression significantly dampened after 3 years post-withdrawal (e.g. *CD52*, *CD68*, *STAT1* and *GPNMB*) (Table 4, Fig. 3B). In comparison, the expression of *CXCL10*, *CXCL9*, *UBD*, *IRF1* and *STAT1* was significantly increased in the liver biopsies collected at the time of rejection in non-tolerant recipients compared to paired pre-weaning levels (Table 4, Suppl. Tab. 3). On the basis of the expression of endothelial-related genes, the inflammatory changes noted in tolerant patients over time were not associated with endothelial damage and/or activation. Thus, *S1PR1*, *RGS5*, *ENPP2*, *MSL3*, *OPN3*, *PAK2*, *CDH5* and *SELP* transcript levels significantly decreased post-withdrawal (Fig. 3C, Table 4).

Discussion

This study offers the first longitudinal assessment of intrahepatic cellular and molecular immune regulatory mechanisms during the development of SOT after human liver transplantation.

The inflammatory changes and Treg enrichment within the graft reported here have also been seen with a much shorter time scale in animal models of spontaneous liver transplant tolerance (5-7, 25). Likewise Gagliani *et al.* found a transient increase of Treg frequencies first in the blood (up to 3 weeks) and later a transient accumulation in islet allografts (day 30), that decreased two-fold by day 150, after a tolerance induction protocol (26). The presence of inflammatory mononuclear infiltrates enriched in Tregs has also been observed in tolerized skin allografts (unpublished data). However, all those changes in animal models occurred relatively early after transplantation fueling the notion that tolerance induction can be achieved quickly after transplantation. Furthermore, tolerance induction in animals was described as a fast and transient process. In contrast, our data of SOT patients creates a different picture of tolerance induction in humans: SOT was more likely to occur in patients with prolonged time (years) after transplantation (18). Expanded portal infiltrates potentially controlled by Tregs was still seen one year post-withdrawal and the down-regulation of endothelial activation and immune response associated genes were just observed three years post-withdrawal. Even at three years inflammatory portal infiltrates were still not resolved suggesting ongoing immunological activity in the graft. However, this did not lead to endothelial activation, rejection, graft fibrosis or development of donor-specific humoral immune responses, suggesting a balanced immune response without graft damage. Our data do not exclude the contribution of other regulatory mechanisms including e.g. other regulatory cell types like Tr1 cells or innate

lymphoid cells at any time point. These observations will be important for future tolerance inducing trials in humans. First, trials need prolonged monitoring with inclusion of protocol graft biopsies. Second, immuno-interventions promoting active immunoregulation within the graft are likely to synergize with the natural tolerogenic pathways elicited following immunosuppression discontinuation. Third, immunointerventions are more likely to be successful after a long period of time following transplantation.

Although the observation that FOXP3⁺ cells accumulate in the liver grafts of SOT was reported previously (15, 16), the interpretation of the data was compromised by the fact that drug-free patients were compared with liver recipients on calcineurin inhibitor-based maintenance IS, which is known to affect Treg numbers (27). Furthermore, longitudinally collected liver biopsy information was not available and Treg/Teff ratios were not described in those previous reports. Although increased Treg numbers does not proof their functional importance in association studies with human samples, we want to point out that Treg accumulation within the graft was important for tolerance in animal models (28). In addition, our method of FOXP3 staining is closely related to the epigenetical Treg detection via the Treg-specific demethylated region (TSDR) and the TSDR methylation status correlated closely with stability and function of true Tregs (29). Our findings also partially resemble what has been described in patients converted from tacrolimus to sirolimus (30). In this study, intrahepatic FOXP3⁺ cells increased following tacrolimus discontinuation, although it is unclear if these changes followed a similar kinetic pattern to what we observed here and whether they were also associated to differences in immune activation and exhaustion gene markers (30).

Due to the limited amount of biomaterial in prospective human studies we cannot provide data of functionality and allo-reactivity of the adaptive immune system. Only a small number of immune cell subsets can be analyzed in graft biopsies, and direct in-vitro assays if global functionality cannot be performed when employing conventional clinical liver biopsies. Furthermore, PBMCs do not provide a suitable surrogate, as there are often disparities between intragraft immune responses and those detected in the circulation (20, 21, 23). To overcome these limitations we applied the gene expression analysis that assesses immunological changes of infiltrating cell types and graft stroma cells and correlated the data with the long-term clinical outcome. This is in line with recent results of the molecular microscope approach, in which histological data is complemented with expression data (24).

The bi-phasic changes in graft infiltrating Tregs and intrahepatic expression of immune regulatory as well as endothelial-associated gene expression reported here point to miscellaneous pathways that could be involved in the long-term maintenance of SOT beyond year 1. While the portal infiltrate expansion seen at year 1 is accompanied by an increase of Tregs, this inflammation does not lead to increased transaminases, or rejection suggesting a balanced inflammation. At year three expression analysis points to lower immune activation with less endothelial activation and a return of Treg numbers to baseline. As the immune infiltrates did not disappear, this could involve other tolerance mechanisms such as immune exhaustion (25). In this regard it is also interesting to note that there was a trend to an increased CD4⁺/CD8⁺ ratio in contrast to the decreased CD4⁺/CD8⁺ ratio seen in acute rejection (20).

It is noteworthy that before IS withdrawal no differences in Treg/Teff ratio and pro-inflammatory gene expression were noted between tolerant and non-tolerant

HCV-negative recipients (17). This suggests that sequential analyses are essential to understand the mechanisms at play during SOT acquisition. In this regard, biomarkers predictive of IS withdrawal outcome, rather than a true fingerprint of SOT, are more likely to constitute biomarkers of a state conducive to tolerance once IS drugs are discontinued. The lack of longitudinal changes of the respective T cell populations in peripheral blood supports the notion, that intrahepatic immunological changes are not mirrored in the blood (20, 21, 23). This emphasizes the need to access the allograft itself to accurately monitor the SOT state.

In short, we report here for the first time that in human liver transplant recipients SOT is characterized by persistent portal infiltrates with a benign clinical course without longitudinal evidence of relevant graft damages. This histological pattern points to a long-lasting immunological interplay of the recipient with the graft, which involves early increased Treg numbers and later a down-regulation of immune response genes.

Our data has important clinical and mechanistic implications for the design of future diagnostic and therapeutic clinical studies aiming at the achievement of allograft tolerance clinical organ transplantation.

Acknowledgements

The work was supported by grants from the German Research Foundation (SFB738 project B4 and SFB TR127 project A4), the cluster of excellence REBIRTH, the Integrated Research Center Transplantation (IFB-Tx projects CBT3, ISI5 and ISI6) funded by the German Federal Ministry of Education and Research (reference number: 01EO0802 and 01EO1302), the Instituto de Salud Carlos III Spain (FISS 1881/2011), and by the National Institute for Health Research (NIHR) Biomedical Research Centre based at Guy's and St Thomas' National Health Service (NHS) Foundation Trust and King's College London. R.T. was supported by the Young Faculty Program from the Hannover Medical School.

Disclosure

The authors of this manuscript have no conflicts of interest to disclose as described by the American Journal of Transplantation.

Table 1. Baseline characteristics of the patients included in the study

Characteristic	Tolerant group n=24	Non-tolerant group N=14
	mean ± SD	mean ± SD
Age at weaning start (years)	60.7±10.9	58.4±7.8
Gender (% male)	83.3	64.3
Time from transplant to minimization start (months)	137.5±43.6	79.7±28.9
Donor age (years)	36.8±16.3	41.1±22.7
Immunosuppressive therapy at weaning start (no. of patients)		
Tacrolimus	3	7
Cyclosporin A	9	5
Mycophenolate	6	0
Azathioprine	1	0
Tacrolimus + mycophenolate	2	0
Cyclosporin A + mycophenolate	3	2
Liver function tests at weaning start		
Aspartate aminotransferases (U/L)	26.0±9.2	34.7±33.1
Alanine aminotransferases (U/L)	25.5±12.6	37.1±53.1
Gamma-glutamyl transpeptidase (U/L)	47.3±43.7	37.2±43.7
Alkaline phosphatase (U/L)	168.2±72	153.8±67.9

*All patients were HCV-RNA undetectable at the time of weaning

Table 2: Intrahepatic immunophenotyping of portal infiltrates liver biopsies of non-HCV patients before and after weaning of immunosuppressants.

	pre-weaning	1 year SOT	3 years SOT	Global p-value	1 y SOT vs pre-weaning	3 y SOT vs 1 y SOT	3y SOT vs pre-weaning
	mean (SD)	mean (SD)	mean (SD)		p-value (diff.) ¹	p-value (diff.) ¹	p-value (diff.) ¹
Number of biopsies	15	14	12				
Infiltrate size [mm ²]	0.018 (0.009)	0.029 (0.016)	0.041 (0.027)	0.002	0.032 (1.67)	0.35 (1.40)	0.0002 (2.33)
CD4 ⁺ density [cells per mm ²]	1304 (407)	1511 (559)	1475 (702)	0.72	1.00 (1.07)	1.00 (0.94)	1.00 (1.01)
CD8 ⁺ density [cells per mm ²]	988 (365)	1089 (366)	923 (423)	0.41	1.00 (1.04)	0.55 (0.83)	0.95 (0.86)
CD4 ⁺ FOXP3 ⁺	44 (25)	62 (26)	47 (41)	0.042	0.038 (1.44)	0.095	1.00

density [cells per mm ²]						(0.66)	(0.96)
CD4 ⁺ / CD8 ⁺ ratio	1.41 (0.40)	1.41 (0.29)	1.60 (0.28)	0.26	1.00 (1.02)	0.42 (1.14)	0.39 (1.16)
Treg / CD4 ⁺ + CD8 ⁺ ratio	0.019 (0.011)	0.024 (0.009)	0.018 (0.010)	0.064	0.33 (1.34)	0.041 (0.71)	1.00 (0.96)
Treg / CD4 ⁺ ratio	0.034 (0.020)	0.043 (0.018)	0.029 (0.016)	0.021	0.11 (1.33)	0.009 (0.66)	0.94 (0.88)
Treg / CD8 ⁺ ratio	0.047 (0.027)	0.057 (0.018)	0.046 (0.026)	0.15	0.42 (1.35)	0.15 (0.77)	1.00 (1.04)

(diff)¹ – estimated fold-differences between the group means derived from linear mixed-effects models of log-transformed data. P-values refer to analysis with linear mixed-effects models of non-transformed data except for infiltrate size, where log-transformation was used to correct for skewness of the distribution. Significant values (p<0.05) are highlighted in bold. Abbreviations: SOT: spontaneous operational tolerance.

Table 3: Flow cytometric analysis of PBMC of non-HCV patients before and after weaning of immunosuppressants.

	pre-weaning mean (SD)	1 year SOT mean (SD)	3 years SOT mean (SD)	Global p-value
Number of samples	6*	12	5**	
CD3 ⁺ % of lymphocytes	68.2 (12.4)	72.1 (7.4)	<i>nd</i>	0.16
CD4 ⁺ % of CD3 ⁺	50.5 (8.1)	44 (16.2)	40.2 (12.9)	0.37
CD8 ⁺ % of CD3 ⁺	28.3 (8.2)	31.1 (7.7)	<i>nd</i>	0.15
CD4 ⁺ CD25 ⁺ FOXP3 ⁺ % of CD4 ⁺	7.1 (2.5)	5.8 (2.4)	5.5 (1.9)	0.097
CD4 ⁺ / CD8 ⁺ ratio	1.9 (0.6)	1.6 (1.0)	<i>nd</i>	0.25

* n=9 for CD4⁺CD25⁺FOXP3⁺%; ** n=7 for CD4⁺CD25⁺FOXP3⁺%. Abbreviations: *nd*: not determined; SOT: spontaneous operational tolerance.

Table 4: Significant differences in gene expression in sequentially collected liver tissue samples

	Gene	Official name	Longitudinal analysis of SOT patients				Rejection vs pre-Weaning
			Global p-value	1 year SOT vs pre-Weaning	3 years SOT vs 1 year SOT	3 year SOT vs pre-Weaning	
Immuno-regulation markers	CD244	CD244 molecule, natural killer cell receptor 2B4	0.018	1.01 (1.00)	-1.46 (0.042)	-1.44 (0.016)	<i>nd</i>
	FOXP3	forkhead box P3	0.009	2.25 (0.013)	-2.52 (0.003)	-1.12 (1.00)	1.74 (0.006)
rejection markers	CD52	CD52 molecule	0.004	-1.13 (1.00)	-1.58 (0.037)	-1.78 (0.0008)	-1.21 (0.29)
	CXCL10	chemokine (C-X-C motif) ligand 10	0.22	1.15 (1.00)	-1.46 (0.26)	-1.27 (0.64)	1.77 (0.004)
	CXCL9	chemokine (C-X-C motif) ligand 9	0.17	1.54 (0.30)	-1.62 (0.19)	-1.05 (1.00)	1.72 (0.009)
	GPNMB	glycoprotein (transmembrane) nmb	0.039	1.39 (0.20)	-1.63 (0.018)	-1.18 (0.87)	1.03 (0.98)
	IL32	interleukin 32	0.040	1.81 (0.020)	-1.56 (0.13)	1.16 (1.00)	1.08 (0.28)
	IRF1	interferon regulatory factor 1	0.27	1.37 (0.40)	-1.38 (0.39)	-1.00 (1.00)	1.19 (0.027)
	STAT1	signal transducer and activator of transcription 1	0.038	1.51 (0.18)	-1.83 (0.017)	-1.22 (0.92)	1.37 (0.008)
	UBD	ubiquitin D	0.066	2.04 (0.069)	-1.99 (0.082)	1.03 (1.00)	2.98 (0.016)
	thelium cell markers	CDH5	cadherin 5, type 2	0.038	1.3 (0.10)	-1.40 (0.020)	-1.07 (1.00)
ENPP2		ectonucleotide pyrophosphatase/phosphodiesterase 2	0.001	1.09 (1.00)	-1.70 (0.0006)	-1.57 (0.0006)	<i>nd</i>
MSL3		male-specific lethal 3 homolog	0.022	1.12 (1.00)	-1.67 (0.022)	-1.50 (0.047)	<i>nd</i>
OPN3		opsin 3	<0.0001	1.08 (0.80)	-1.39 (<0.0001)	-1.29 (<0.0001)	<i>nd</i>
PAK2		p21 protein (Cdc42/Rac)-activated kinase 2	0.043	-1.02 (1.00)	-1.15 (0.17)	-1.17 (0.033)	<i>nd</i>

<i>RGS5</i>	regulator of G-protein signaling 5	0.0041	-1.74 (0.10)	-1.34 (0.78)	-2.32 (0.0006)	<i>nd</i>
<i>S1PR1</i>	sphingosine-1-phosphate receptor 1	0.013	-1.43 (0.095)	-1.11 (1.00)	-1.58 (0.005)	<i>nd</i>
<i>SELP</i>	selectin P	0.021	1.12 (1.00)	-1.60 (0.019)	-1.43 (0.050)	<i>nd</i>

Estimated fold differences are derived from linear mixed-effects models for the SOT groups and from the ratio of the group means for Rejection vs paired pre-Weaning comparison following the $2^{-\Delta\Delta CT}$ method. Global p-values (derived from likelihood ratio tests) evaluate the association between timepoint and gene expression. In brackets are shown p-values from multiple comparisons with Bonferroni correction (for SOT groups) or from paired t-tests for the comparison of Rejection vs pre-Weaning groups. Significant values ($p < 0.05$) are highlighted in bold. Abbreviations: *nd*: not determined; SOT: spontaneous operational tolerance.

Figure legends

Figure 1: Multicolor immunofluorescence of human FFPE liver biopsies.

(A) Representative histology from a tolerant patient at year 3 after successful IS withdrawal. Co-stainings for CD4 (green), CD8 (blue), FOXP3 (red), DAPI (white) of intrahepatic T cell infiltration were performed in FFPE liver biopsy section. Liver sinusoidal epithelial cells weakly express CD4 and can be distinguished from T cells by strength of CD4 expression, shape and localization of cells. The white line surrounds areas of portal infiltrations and excludes lumen of veins, arteries and bile ducts. (B) Secondary reagent control of representative portal tract in another biopsy from a tolerant patient. Autofluorescence and unspecific hepatocellular cytoplasmic staining (red) that resulted from biotin-streptavidin interaction in biotin rich hepatocytes caused the red-orange staining of hepatocytes. White dots are mostly autofluorescent erythrocytes. (C) Higher magnification of portal infiltrates with clear nuclear localization of the FOXP3 in CD4⁺ cells as demonstrate by (D) DAPI counterstaining (white) in higher magnification. White bars represent 100 μm (A, B) or 20 μm (C, D).

Figure 2: Transient changes of the portal T cell compartment after successful immunosuppressant withdrawal.

(A) Size of portal infiltrates in protocol liver biopsies before, 1 and 3 years after complete and successful immunosuppressant weaning. (B) Portal infiltration density of CD4⁺FOXP3⁺ Tregs. (C) Portal Tregs/CD4⁺ ratio. (D) Portal CD4⁺ (white bars) and CD8⁺ (grey bars) T cell infiltration densities. (E) Mean relative changes of immunophenotyping during SOT liver biopsies and blood samples. Portal Tregs/CD4⁺ ratio (black line), peripheral blood Tregs/CD4⁺ ratio (grey line), portal infiltrate size (black dotted line), portal CD4⁺/CD8⁺ ratio (black dashed line).

Sample numbers for SOT groups are shown in Table 2. Statistical analyses of SOT groups were carried out with linear mixed-effects models. P-values were adjusted with Bonferroni correction for multiple comparisons. Data for infiltrate size were log-transformed (ln) in order to correct for skewness of the distribution. Spontaneous operational tolerance (SOT).

Figure 3: Sequential changes in intrahepatic transcriptional markers in liver recipients undergoing immunosuppression withdrawal.

Relative expression of *FOXP3*, *CD244*, *PD1* and *BATF* (A), *IL32*, *CD68*, *STAT1*, *GPNUMB* and *CD52* (B), and *CDH5*, *ENPP2*, *OPN3*, *PAK2*, *S1PR1*, *RGS5*, *SELP* and *MSL3* (C) in liver tissue samples collected from liver recipients before the initiation of IS weaning (pre-weaning), 1 year after complete IS discontinuation (1 year SOT), and 3 years after complete IS discontinuation (3 years SOT). Data were obtained on a Fluidigm real-time PCR platform and are displayed as mean and standard deviation of $-\Delta C_Q$. * $p < 0.05$; ** $p < 0.01$.

Supplementary Material

Supplementary Table 1: Availability of patient material for longitudinal immunophenotyping and gene expression analysis of SOT.

	IF pre-weaning	IF 1 year SOT	IF 3 years SOT	Lbx 5 years SOT	PBMC	Gene expression
Pat. 1	+	+	+		+	+
Pat. 2	+		+	+		+
Pat. 3	+		+	+	+	+
Pat. 4	+	+	+		+	+
Pat. 5	+	+	+		+	+
Pat. 6	+			+		
Pat. 7	+					+
Pat. 8	+	+	+		+	
Pat. 9	+	+	+		+	
Pat. 10	+	+	+	+	+	+
Pat. 11	+	+			+	+
Pat. 12	+	+			+	
Pat. 13	+	+	+		+	+
Pat. 14	+	+			+	+
Pat. 15	+	+			+	+
Pat. 16		+	+	+		
Pat. 17		+	+			
Pat. 18		+	+			
Pat. 19						+
Pat. 20						+
Pat. 21						+
Pat. 22						+
Pat. 23						+
Pat. 24						+

Abbreviations: SOT: spontaneous operational tolerance; Pat.: patient; IF: Immunofluorescence;

Lbx: liver biopsy; PBMC: peripheral blood mononuclear cells.

Supplementary Table 2: Liver Histopathology Findings *

Histological Evaluation	pre-weaning	1 year SOT	3 years SOT	paired ANOVA
	mean (range)	mean (range)	mean (range)	
Lobular inflammation	0 (0-1)	0 (0-1)	1 (0-1)	0.186
Central perivenulitis	0	0 (0-1)	0 (0-1)	0.585
Portal inflammation	1 (0-2)	1 (0-1)	1 (0-1)	0.618
Interface hepatitis	0 (0-1)	0 (0-1)	0	0.585
Biliary lesions	0 (0-1)	0 (0-1)	0 (0-1)	0.682
Bile duct loss	0	0	0 (0-1)	0.363
Portal vein endothelitis	0 (0-1)	0 (0-1)	0 (0-1)	0.682
Portal fibrosis	1 (0-1)	0 (0-1)	0 (0-3)	0.478
Perisinusoidal fibrosis	0 (0-2)	0 (0-2)	1 (0-2)	0.187

* Data correspond to a central pathology analysis of liver transplant recipients in whom all 3 sequential liver biopsies (pre-weaning, 1 year SOT and 3 years SOT) were available for evaluation (n=7 each). Spontaneous operational tolerance (SOT).

Lobular inflammation: 0=no; 1=mild (sinusoidal cells and/or mild focal necrosis); 2=moderate (multiple necro-inflammatory foci); 3=marked (confluent or bridging necrosis). Central perivenulitis (with or without endothelitis): 0=no; 1=mild (patchy, focal perivenular inflammation); 2=moderate (perivenulitis in most central veins); 3=marked (confluent or bridging hepatocellular necrosis). Portal inflammation: 0=no; 1=mild (small groups of inflammatory cells); 2=moderate (>50% of portal tracts, expansive); 3=marked. Interface hepatitis: 0=no; 1=mild; 2=moderate; 3=severe. Bile duct lesions: 0=no; 1=minimal (intraepithelial inflammatory cells or abnormal colangiocytes); 2=moderate (epithelial lesions in most of portal tracts, no destruction); 3=marked. Bile duct loss: 0=no; 1=<50%; 2=>50%. Portal vein endothelitis: 0=no; 1=mild (minority of portal veins); 2=mild (most of the portal veins); 3=marked. Portal fibrosis: 0=no; 1=minimal (minority of portal tracts); 2=moderate (most of the portal tracts, periportal expansion); 3=bridging fibrosis; 4=cirrhosis. Perisinusoidal fibrosis: 0=no; 1=Focal patchy; 2=Prominent.

Abbreviations: SOT: spontaneous operational tolerance.

Supplementary Table 3: Differences in gene expression in sequentially collected liver biopsy and PBMCTissue samples for longitudinal analysis of SOT.

	Gene	Official name	Longitudinal analysis of SOT patients				Rejection vs pre-Weaning
			Global p-value	1 year SOT vs pre-Weaning	3 years SOT vs 1 year SOT	3 year SOT vs pre-Weaning	
Immunoregulation markers	CD244	CD244 molecule, natural killer cell receptor 2B4	0.018	1.01 (1.00)	-1.46 (0.042)	-1.44 (0.016)	<i>nd</i>
	<i>CD274</i>	CD274 molecule	0.077	1.07 (1.00)	-1.34 (0.096)	-1.25 (0.18)	<i>nd</i>
	<i>CD3</i>	CD3e molecule, epsilon	0.61	1.36 (1.00)	-1.40 (1.00)	-1.03 (1.00)	<i>nd</i>
	<i>CTLA4</i>	cytotoxic T-lymphocyte-associated protein 4	0.72	1.16 (1.00)	-1.37 (1.00)	-1.18 (1.00)	<i>nd</i>
	FOXP3	forkhead box P3	0.009	2.25 (0.013)	-2.52 (0.003)	-1.12 (1.00)	1.74 (0.006)
	<i>IL10</i>	interleukin 10	0.70	1.17 (1.00)	-1.39 (1.00)	-1.18 (1.00)	<i>nd</i>
	<i>LAG3</i>	lymphocyte-activation gene 3	0.37	1.50 (0.51)	-1.41 (0.72)	1.07 (1.00)	<i>nd</i>
	<i>PD1</i>	arogenate dehydratase 3	0.054	1.59 (0.21)	-1.92 (0.030)	-1.21 (1.00)	<i>nd</i>
	<i>TIM3</i>	hepatitis A virus cellular receptor 2 (HAVCR2)	0.089	1.09 (1.00)	-1.52 (0.12)	-1.39 (0.19)	<i>nd</i>
	<i>BATF</i>	basic leucine zipper transcription factor, ATF-like	0.074	1.52 (0.32)	-1.86 (0.047)	-1.22 (1.00)	<i>nd</i>
Rejection markers	<i>CD19</i>	CD19 molecule	0.56	-1.24 (1.00)	-1.29 (1.00)	-1.60 (0.84)	<i>nd</i>
	<i>CD34</i>	CD34 molecule	0.10	-1.08 (1.00)	-1.30 (0.45)	-1.41 (0.090)	<i>nd</i>
	<i>CD68</i>	CD68 molecule	0.050	1.26 (0.57)	-1.57 (0.029)	-1.25 (0.42)	<i>nd</i>
	<i>CCL19</i>	chemokine (C-C motif) ligand 19	0.19	-1.47 (0.87)	-1.24 (1.00)	-1.83 (0.18)	1.14 (0.82)
	CD52	CD52 molecule	0.004	-1.13	-1.58	-1.78	-1.21 (0.29)

				(1.00)	(0.037)	(0.0008)	
	<i>CD8A</i>	CD8a molecule	0.39	1.35 (1.00)	-1.54 (0.49)	-1.14 (1.00)	1.06 (0.38)
	<i>CXCL10</i>	chemokine (C-X-C motif) ligand 10	0.22	1.15 (1.00)	-1.46 (0.26)	-1.27 (0.64)	1.77 (0.004)
	<i>CXCL9</i>	chemokine (C-X-C motif) ligand 9	0.17	1.54 (0.30)	-1.62 (0.19)	-1.05 (1.00)	1.72 (0.009)
	<i>DHRS9</i>	dehydrogenase/reductase (SDR family) member 9	0.086	1.68 (0.11)	-1.69 (0.099)	-1.01 (1.00)	1.28 (0.13)
	<i>GBP2</i>	guanylate binding protein 2, interferon-inducible	0.33	1.18 (0.69)	-1.23 (0.41)	-1.04 (1.00)	1.05 (0.59)
	<i>GPNMB</i>	glycoprotein (transmembrane) nmb	0.039	1.39 (0.20)	-1.63 (0.018)	-1.18 (0.87)	1.03 (0.98)
	<i>IL18BP</i>	interleukin 18 binding protein	0.18	1.09 (1.00)	-1.43 (0.26)	-1.31 (0.41)	-1.08 (0.90)
	<i>IL32</i>	interleukin 32	0.040	1.81 (0.020)	-1.56 (0.13)	1.16 (1.00)	1.08 (0.28)
	<i>IRF1</i>	interferon regulatory factor 1	0.27	1.37 (0.40)	-1.38 (0.39)	-1.00 (1.00)	1.19 (0.027)
	<i>LYZ</i>	lysozyme (renal amyloidosis)	0.32	1.13 (1.00)	-1.29 (0.38)	-1.14 (1.00)	1.21 (0.20)
	<i>MMP9</i>	matrix metalloproteinase 9	0.44	1.46 (0.73)	-1.45 (0.73)	1.01 (1.00)	1.03 (0.97)
	<i>STAT1</i>	signal transducer and activator of transcription 1	0.038	1.51 (0.18)	-1.83 (0.017)	-1.22 (0.92)	1.37 (0.008)
	<i>TAP1</i>	transporter 1, ATP-binding cassette, sub-family B (MDR/TAP)	0.075	1.46 (0.082)	-1.45 (0.092)	1.01 (1.00)	1.19 (0.094)
	<i>TOP2A</i>	topoisomerase (DNA) II alpha	0.10	1.51 (0.68)	-2.13 (0.076)	-1.41 (0.74)	1.29 (0.22)
	<i>UBD</i>	ubiquitin D	0.066	2.04 (0.069)	-1.99 (0.082)	1.03 (1.00)	2.98 (0.016)
Endothelial cell markers	<i>ADCY4</i>	adenylate cyclase 4	0.39	1.16 (1.00)	-1.32 (0.49)	-1.14 (1.00)	<i>nd</i>
	<i>CDH5</i>	cadherin 5, type 2	0.038	1.3 (0.10)	-1.40 (0.020)	-1.07 (1.00)	<i>nd</i>

<i>COL4A1</i>	collagen, type IV, alpha 1	0.52	1.22 (1.00)	-1.25 (0.81)	-1.03 (1.00)	<i>nd</i>
<i>ENPP2</i>	ectonucleotide pyrophosphatase/phosphodiesterase 2	0.001	1.09 (1.00)	-1.70 (0.0006)	-1.57 (0.0006)	<i>nd</i>
<i>HSPG2</i>	heparan sulfate proteoglycan 2	0.66	1.08 (1.00)	-1.11 (1.00)	-1.03 (1.00)	<i>nd</i>
<i>IGFBP7</i>	insulin-like growth factor binding protein 7	0.19	-1.08 (1.00)	-1.25 (0.71)	-1.35 (0.20)	<i>nd</i>
<i>LAMB1</i>	laminin, beta 1	0.53	-1.04 (1.00)	-1.12 (1.00)	-1.16 (0.81)	<i>nd</i>
<i>MFNG</i>	MFNG O-fucosylpeptide 3-beta-N-acetylglucosaminyltransferase	0.14	1.19 (1.00)	-1.44 (0.12)	-1.22 (0.64)	<i>nd</i>
<i>MLL3</i>	myeloid/lymphoid or mixed-lineage leukemia 3	0.22	1.15 (0.29)	-1.14 (0.33)	1.01 (1.00)	<i>nd</i>
<i>MSL3</i>	male-specific lethal 3 homolog	0.022	1.12 (1.00)	-1.67 (0.022)	-1.50 (0.047)	<i>nd</i>
<i>OPN3</i>	opsin 3	<0.0001	1.08 (0.80)	-1.39 (<0.0001)	-1.29 (<0.0001)	<i>nd</i>
<i>PAK2</i>	p21 protein (Cdc42/Rac)-activated kinase 2	0.043	-1.02 (1.00)	-1.15 (0.17)	-1.17 (0.033)	<i>nd</i>
<i>RGS5</i>	regulator of G-protein signaling 5	0.0041	-1.74 (0.10)	-1.34 (0.78)	-2.32 (0.0006)	<i>nd</i>
<i>S1PR1</i>	sphingosine-1-phosphate receptor 1	0.013	-1.43 (0.095)	-1.11 (1.00)	-1.58 (0.005)	<i>nd</i>
<i>SELP</i>	selectin P	0.021	1.12 (1.00)	-1.60 (0.019)	-1.43 (0.050)	<i>nd</i>
<i>TRPV2</i>	transient receptor potential cation channel, subfamily V, member 2	0.21	1.39 (0.21)	-1.27 (0.56)	1.09 (1.00)	<i>nd</i>

Estimated fold differences are derived from linear mixed-effects models for the SOT groups and from the ratio of the group means for Rejection vs paired pre-Weaning comparison following the 2^{ΔΔCT} method. Global p-values (derived from likelihood ratio tests) evaluate the association between timepoint and gene expression. In brackets are shown p-values from multiple comparisons with Bonferroni correction (for SOT groups) or from paired t-tests for the comparison of Rejection vs

pre-Weaning groups. Significant values ($p < 0.05$) are highlighted in bold. Abbreviations: *nd*: not determined; SOT: spontaneous operational tolerance.

Supplementary Figure 1: Representative flow cytometry and gating strategy for sequentially collected blood samples.

References

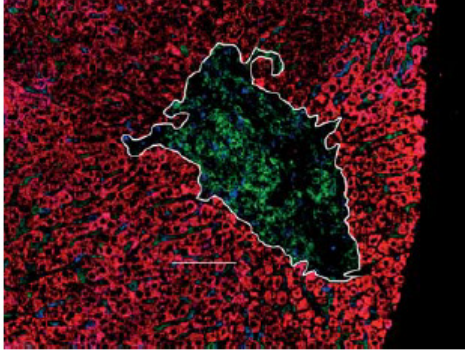
1. Gelson W, Hoare M, Dawwas MF, Vowler S, Gibbs P, Alexander G. The pattern of late mortality in liver transplant recipients in the United Kingdom. *Transplantation*. 2011 Jun 15;91(11):1240-4. PubMed PMID: 21516069.
2. Di Cocco P, Bonanni L, D'Angelo M, Clemente K, Greco S, Rizza V, et al. Clinical operational tolerance after solid organ transplantation. *Transplant Proc*. 2009 May;41(4):1278-82. PubMed PMID: 19460538.
3. Knechtle SJ, Kwun J. Unique aspects of rejection and tolerance in liver transplantation. *Semin Liver Dis*. 2009 Feb;29(1):91-101. PubMed PMID: 19235662.
4. Sanchez-Fueyo A. Hot-topic debate on tolerance: immunosuppression withdrawal. *Liver Transpl*. 2011 Nov;17 Suppl 3:S69-73. PubMed PMID: 21850680.
5. Crispe IN. Hepatic T cells and liver tolerance. *Nat Rev Immunol*. 2003 Jan;3(1):51-62. PubMed PMID: 12511875.
6. Benseler V, McCaughan GW, Schlitt HJ, Bishop GA, Bowen DG, Bertolino P. The liver: a special case in transplantation tolerance. *Semin Liver Dis*. 2007 May;27(2):194-213. PubMed PMID: 17520518.
7. Li W, Kuhr CS, Zheng XX, Carper K, Thomson AW, Reyes JD, et al. New insights into mechanisms of spontaneous liver transplant tolerance: the role of Foxp3-expressing CD25+CD4+ regulatory T cells. *Am J Transplant*. 2008 Aug;8(8):1639-51. PubMed PMID: 18557727.
8. Alex Bishop G, Bertolino PD, Bowen DG, McCaughan GW. Tolerance in liver transplantation. *Best practice & research Clinical gastroenterology*. 2012 Feb;26(1):73-84. PubMed PMID: 22482527.
9. Martinez-Llordella M, Puig-Pey I, Orlando G, Ramoni M, Tisone G, Rimola A, et al. Multiparameter immune profiling of operational tolerance in liver transplantation. *Am J Transplant*. 2007 Feb;7(2):309-19. PubMed PMID: 17241111.
10. Li Y, Koshiba T, Yoshizawa A, Yonekawa Y, Masuda K, Ito A, et al. Analyses of peripheral blood mononuclear cells in operational tolerance after pediatric living donor liver transplantation. *Am J Transplant*. 2004 Dec;4(12):2118-25. PubMed PMID: 15575917.
11. Ohe H, Waki K, Yoshitomi M, Morimoto T, Nafady-Hego H, Satoda N, et al. Factors affecting operational tolerance after pediatric living-donor liver transplantation: impact of early post-transplant events and HLA match. *Transpl Int*. 2012 Jan;25(1):97-106. PubMed PMID: 22117557.
12. Tokita D, Mazariegos GV, Zahorchak AF, Chien N, Abe M, Raimondi G, et al. High PD-L1/CD86 ratio on plasmacytoid dendritic cells correlates with elevated T-regulatory cells in liver transplant tolerance. *Transplantation*. 2008 Feb 15;85(3):369-77. PubMed PMID: 18301333.
13. Mazariegos GV, Zahorchak AF, Reyes J, Chapman H, Zeevi A, Thomson AW. Dendritic cell subset ratio in tolerant, weaning and non-tolerant liver recipients is not affected by extent of immunosuppression. *Am J Transplant*. 2005 Feb;5(2):314-22. PubMed PMID: 15643991.
14. Castellaneta A, Mazariegos GV, Nayyar N, Zeevi A, Thomson AW. HLA-G level on monocytoid dendritic cells correlates with regulatory T-cell Foxp3 expression in liver transplant tolerance. *Transplantation*. 2011 May 27;91(10):1132-40. PubMed PMID: 21423069.

15. Yoshitomi M, Koshiba T, Haga H, Li Y, Zhao X, Cheng D, et al. Requirement of protocol biopsy before and after complete cessation of immunosuppression after liver transplantation. *Transplantation*. 2009 Feb 27;87(4):606-14. PubMed PMID: 19307800.
16. Li Y, Zhao X, Cheng D, Haga H, Tsuruyama T, Wood K, et al. The presence of Foxp3 expressing T cells within grafts of tolerant human liver transplant recipients. *Transplantation*. 2008 Dec 27;86(12):1837-43. PubMed PMID: 19104431.
17. Bohne F, Martinez-Llordella M, Lozano JJ, Miquel R, Benitez C, Londono MC, et al. Intra-graft expression of genes involved in iron homeostasis predicts the development of operational tolerance in human liver transplantation. *J Clin Invest*. 2012 Jan 3;122(1):368-82. PubMed PMID: 22156196.
18. Benitez C, Londono MC, Miquel R, Manzia TM, Abraldes JG, Lozano JJ, et al. Prospective multi-center clinical trial of immunosuppressive drug withdrawal in stable adult liver transplant recipients. *Hepatology*. 2013 Mar 26. PubMed PMID: 23532679.
19. Feng S, Ekong UD, Lobritto SJ, Demetris AJ, Roberts JP, Rosenthal P, et al. Complete immunosuppression withdrawal and subsequent allograft function among pediatric recipients of parental living donor liver transplants. *Jama*. 2012 Jan 18;307(3):283-93. PubMed PMID: 22253395.
20. Taubert R, Pischke S, Schlue J, Wedemeyer H, Noyan F, Heim A, et al. Enrichment of regulatory T cells in acutely rejected human liver allografts. *Am J Transplant*. 2012 Dec;12(12):3425-36. PubMed PMID: 22994589.
21. He Q, Fan H, Li JQ, Qi HZ. Decreased circulating CD4+CD25highFoxp3+ T cells during acute rejection in liver transplant patients. *Transplant Proc*. 2011 Jun;43(5):1696-700. PubMed PMID: 21693260.
22. Issa F, Hester J, Milward K, Wood KJ. Homing of regulatory T cells to human skin is important for the prevention of alloimmune-mediated pathology in an in vivo cellular therapy model. *PLoS One*. 2012;7(12):e53331. PubMed PMID: 23300911.
23. Taubert R, Hardtke-Wolenski M, Noyan F, Wilms A, Baumann AK, Schlue J, et al. Intrahepatic regulatory T cells in autoimmune hepatitis are associated with treatment response and depleted with current therapies. *J Hepatol*. 2014 Nov;61(5):1106-14. PubMed PMID: 24882050.
24. Sis B, Jhangri GS, Bunnag S, Allanach K, Kaplan B, Halloran PF. Endothelial gene expression in kidney transplants with alloantibody indicates antibody-mediated damage despite lack of C4d staining. *Am J Transplant*. 2009 Oct;9(10):2312-23. PubMed PMID: 19681822.
25. Bohne F, Londono MC, Benitez C, Miquel R, Martinez-Llordella M, Russo C, et al. HCV-Induced Immune Responses Influence the Development of Operational Tolerance After Liver Transplantation in Humans. *Science translational medicine*. 2014 Jun 25;6(242):242ra81. PubMed PMID: 24964989.
26. Gagliani N, Gregori S, Jofra T, Valle A, Stabilini A, Rothstein DM, et al. Rapamycin combined with anti-CD45RB mAb and IL-10 or with G-CSF induces tolerance in a stringent mouse model of islet transplantation. *PLoS One*. 2011;6(12):e28434. PubMed PMID: 22174806.
27. Wekerle T. T-regulatory cells-what relationship with immunosuppressive agents? *Transplant Proc*. 2008 Dec;40(10 Suppl):S13-6. PubMed PMID: 19100898.

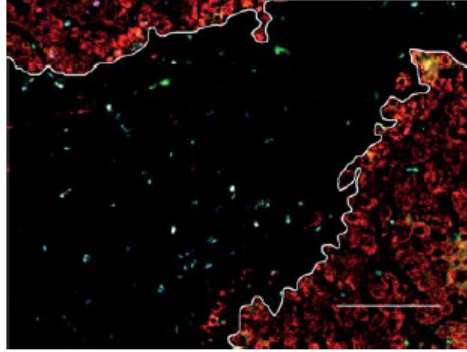
28. Sagoo P, Lombardi G, Lechler RI. Relevance of regulatory T cell promotion of donor-specific tolerance in solid organ transplantation. *Frontiers in immunology*. 2012;3:184. PubMed PMID: 22811678. Pubmed Central PMCID: 3395995.
29. Miyara M, Yoshioka Y, Kitoh A, Shima T, Wing K, Niwa A, et al. Functional delineation and differentiation dynamics of human CD4+ T cells expressing the FoxP3 transcription factor. *Immunity*. 2009 Jun 19;30(6):899-911. PubMed PMID: 19464196.
30. Levitsky J, Mathew JM, Abecassis M, Tambur A, Leventhal J, Chandrasekaran D, et al. Systemic immunoregulatory and proteogenomic effects of tacrolimus to sirolimus conversion in liver transplant recipients. *Hepatology*. 2012 Jan 11. PubMed PMID: 22234876.

Fig. 1

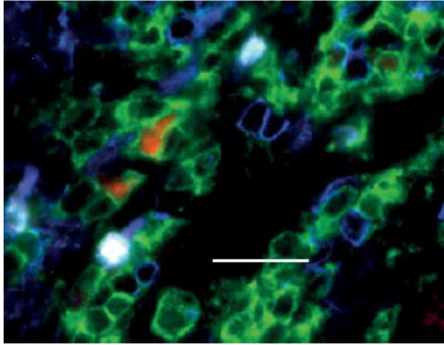
A



B



C



D

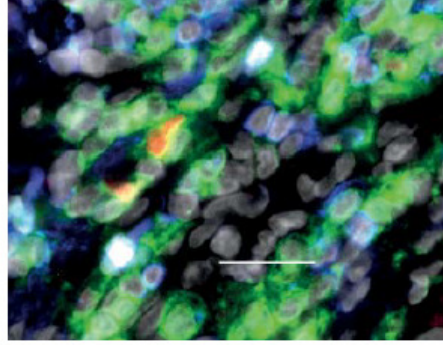


Fig. 2

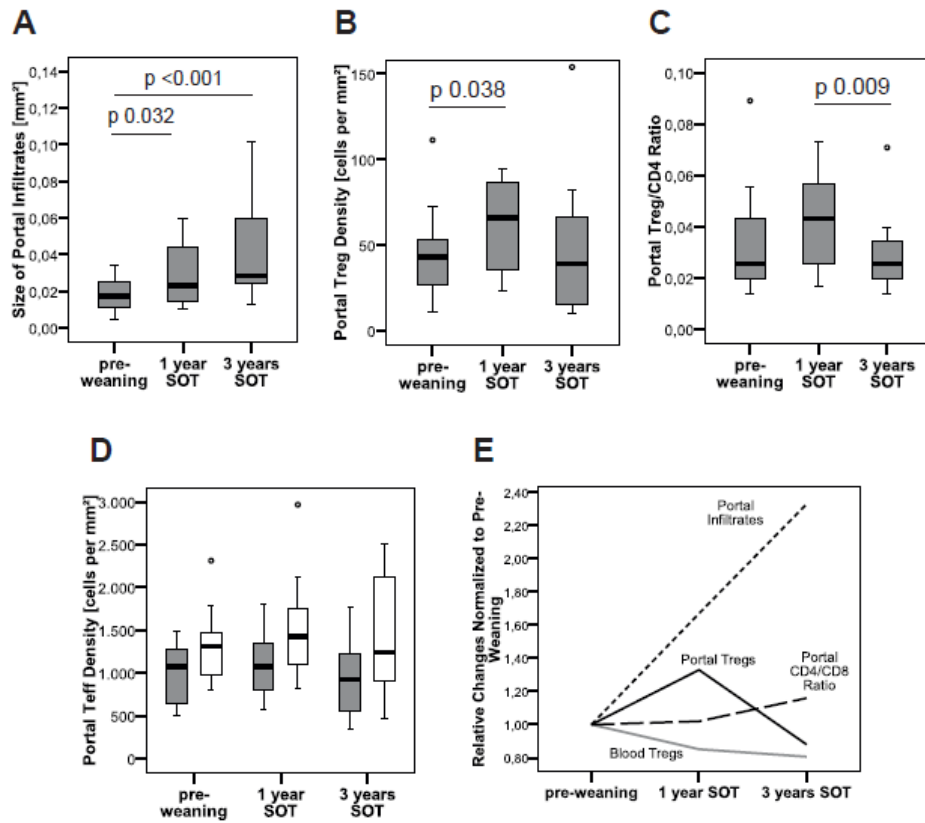
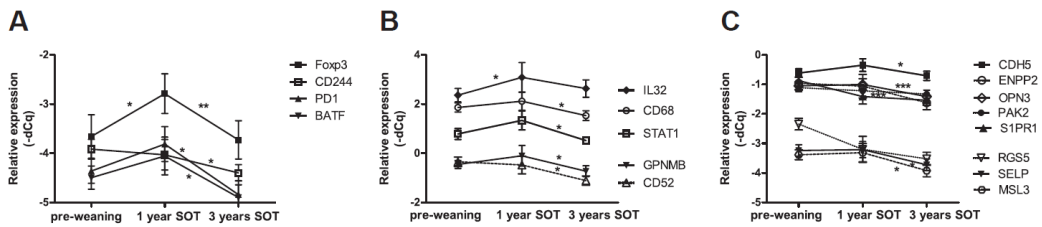


Fig. 3



Suppl. Fig. 1

